IPP-Report

IPP Max-Planck-Institut für Plasmaphysik

Dario Correa-Restrepo

Resistive ballooning modes near the edge of toroidal configurations

IPP 5/80
August 1998

Resistive ballooning modes near the edge of toroidal configurations

Darío Correa-Restrepo

Max-Planck-Institut für Plasmaphysik EURATOM Association, D-85748 Garching, Germany

Abstract

The resistive ballooning mode equations are cast in a new form appropriate for evaluation near the plasma edge of toroidal (axisymmetric as well as three-dimensional) configurations, where the resistive ballooning effects outweigh the diamagnetic effects. Explicit evaluation is carried out for cylindrically symmetric plasmas and for a tokamak model with circular cross-sections. Owing to the large electric resistivity of the regions considered, resistive ballooning modes with growth rates comparable to the characteristic growth rate of ideal ballooning modes are possible. A general feature is that modes with large growth rates are localized around the regions of bad curvature and become less unstable with increasing shear, while those with smaller growth rates are extended along the magnetic field lines and are insensitive to shear.

PACS Numbers: 52.30.Jb, 52.35.g, 52.35.Py .
email: dcr@ipp.mpg.de

I. INTRODUCTION

The purpose of the present paper is to formulate the general ballooning mode equations [1, 2] for conditions valid near the edge of toroidal plasmas, i.e. of axisymmetric tokamaks as well as stellarators. In the region of interest, the ratio α_* of the characteristic electron diamagnetic frequency to the characteristic growth rate of resistive ballooning modes is small, and diamagnetic effects can be neglected [3]. The plasma beta, $\beta = 8\pi p/B^2$, where p is the plasma pressure and B is the magnitude of the magnetic field, is also small, and the electric resistivity is so large that there is a substantial reduction of the stabilizing effect caused by magnetic field line-tying. Under this circumstances, resistive ballooning instabilities can grow on time scales faster than those usually considered and comparable to those of ideal ballooning modes. As far as tokamaks are concerned, and when diamagnetic effects are neglected, it is thus possible to identify the modes which were described as a new branch of resistive ballooning modes in Ref. [4], as modes contained in the usual resistive ballooning equations.

In Sec. II, the resistive ballooning mode equations of Refs. [1, 2] are reformulated. Reference units for time and length which are particularly appropriate to describe the region considered are introduced. This is done in a similar way as in Refs. [4, 5]; the expressions introduced here are, however, valid for general configurations, and not only within the framework of a tokamak model. In Sec. III, general properties properties of the growth rate are derived. In Sec. IV, the results are applied to the case of a cylindrically symmetric plasma. Though this paper is mainly concerned with general configurations, the cylindrical case is particularly clear and illustrative, and it shows general interesting features of the modes. The axisymmetric case is studied in Sec. V with the help of a simple tokamak model, using both analytical and numerical methods. The results are summarized in Sec. VI. A comprehensive derivation of the tokamak model considered is given in Appendix A. The geometric and physical plasma parameters assumed in the axisymmetric case are given in Appendix B.

II. RESISTIVE BALLOONING EQUATIONS

Expressed in Gaussian units, the resistive ballooning mode equations given in Ref. [1, 2], read

$$\frac{\mathrm{d}}{\mathrm{d}y}\left[\frac{\mathrm{C}^2}{B^2\left[1+\left(c^2\alpha^2\eta/4\pi\gamma\right)\mathrm{C}^2\right]}\frac{\mathrm{d}F}{\mathrm{d}y}\right] + \frac{8\pi\dot{p}}{\dot{\chi}^4}\left(\kappa_{\mathrm{v}}+\dot{q}y\kappa_{\varphi}\right)F$$

$$-\frac{4\pi\rho\gamma^2}{\dot{\chi}^2 B^2}\mathbf{C}^2 F \;=\; -\frac{8\pi\dot{p}}{\dot{\chi}^4}\left(\kappa_{\mathrm{v}}+\dot{q}y\kappa_{\varphi}\right)D\;, \tag{1}$$

$$\begin{aligned}&\frac{\mathrm{d}}{\mathrm{d}y}\left[\frac{1}{B^2}\frac{\mathrm{d}D}{\mathrm{d}y}\right]-\frac{\rho\gamma^2}{\dot{\chi}^2}\left[\frac{(\gamma_{\mathrm{H}}p+B^2)}{\gamma_{\mathrm{H}}pB^2}\right]D-\frac{\rho\alpha^2}{\dot{\chi}^2B^2}c^2\eta\gamma\mathbf{C}^2D\\ &-\frac{2\dot{p}}{\dot{\chi}^4}\frac{\alpha^2c^2\eta}{\gamma}\left(\kappa_{\mathrm{v}}+\dot{q}y\kappa_{\varphi}\right)D \;=\; \frac{2\rho}{\dot{p}\dot{\chi}^2}\left(\frac{\dot{p}^2\alpha^2c^2\eta}{\dot{\chi}^2\gamma\rho}+\gamma^2\right)\left(\kappa_{\mathrm{v}}+\dot{q}y\kappa_{\varphi}\right)F\;,\end{aligned} \tag{2}$$

with c the velocity of light.

This representation is based on the coordinates $v,\vartheta,\varphi=\zeta-q_0\vartheta$, where v,ϑ,ζ are Hamada coordinates and $q_0=M/N(M,N$ integers) is the safety factor of an arbitrary reference rational surface. In these coordinates, single-valued physical quantities G satisfy the conditions $G(\vartheta,\varphi)=G(\vartheta,\varphi+1)=G(\vartheta+1,\varphi-M/N)=G(\vartheta+N,\varphi)$, and are thus periodic in ϑ with period N and in φ with period 1. The coordinate y is defined in Fourier-transformed ("ballooning") space and corresponds to the coordinate ϑ in physical space.

The equilibrium magnetic field $\mathbf{B}$ and the gradient along a field line can be then expressed as $\mathbf{B}=\dot{\chi}\left[\boldsymbol{\nabla}\varphi\times\boldsymbol{\nabla}v+(q-q_0)\,\boldsymbol{\nabla}v\times\boldsymbol{\nabla}\vartheta\right]$ and $\mathbf{B}\cdot\boldsymbol{\nabla}=\dot{\chi}\left[\partial_\vartheta+(q-q_0)\,\partial_\varphi\right]$, respectively, with $q=\dot{\psi}/\dot{\chi}$. ψ and χ are the longitudinal and transverse fluxes, respectively. Dots mean derivatives with respect to the volume. Derivation with respect to ϑ corresponds to derivatives along the field line $v=v_0$, $\varphi=\varphi_0$.

Further equilibrium quantities are the pressure p, the density ρ, the (small) resistivity η, the ratio of the specific heats γ_{H} and the curvature $\boldsymbol{\kappa}=\left[(\mathbf{B}/B)\cdot\boldsymbol{\nabla}\right]\mathbf{B}/B$ with covariant components $\kappa_v=\boldsymbol{\kappa}\cdot\boldsymbol{\nabla}\vartheta\times\boldsymbol{\nabla}\varphi$ and $\kappa_\varphi=\boldsymbol{\kappa}\cdot\boldsymbol{\nabla}v\times\boldsymbol{\nabla}\vartheta$, which is the geodesic curvature. The vector $\mathbf{C}$ is defined as $\mathbf{C}=\boldsymbol{\nabla}\varphi-\dot{q}y\boldsymbol{\nabla}v$.

In the ballooning equations, all equilibrium quantities are taken at $v=v_0$, $\varphi=\varphi_0$. The perturbations are described in Fourier space by the quatities F (related to the perturbed electric potential), and D, related to $\boldsymbol{\nabla}\cdot\boldsymbol{\xi}$, where $\boldsymbol{\xi}$ is the usual displacement. The "mode number" α (which is not to be confused with α_* defined in the Introduction) describes the transverse variation of the perturbations with respect to the magnetic field ($\alpha/2\pi$ is essentially the toroidal mode number $n_{\mathrm{tor.}}$ in axial symmetry, but, in addition, it also describes the radial variation of the perturbations). The growth rate γ appears in the original perturbations as $\exp\left[i\gamma t\right]$, and is, in general, a complex quatity.

Length and time normalization units can be introduced by balancing the different terms in these equations. For this purpose, it is convenient to introduce reference quantities, e.g. a mean radius R_0 and the corresponding parallel length $L_{\|0}$,

$$R_0\equiv\frac{\langle B^2\rangle^{1/2}}{2\pi q\left|\dot{\chi}\right|}=\frac{\langle B^2\rangle^{1/2}}{2\pi\left|\dot{\psi}\right|}\;,\quad L_{\|0}\equiv 2\pi qR_0=\frac{\langle B^2\rangle^{1/2}}{\left|\dot{\chi}\right|}\;, \tag{3}$$

the pressure scale length $L_{\rm p}$,

$$L_{\rm p} \equiv -\frac{p}{\dot{p}} \frac{1}{\langle B^2 \rangle^{1/2}} \left\langle \frac{B^2}{|\nabla v|^2} \right\rangle^{1/2} , \tag{4}$$

a characteristic reference curvature $\kappa_{\rm v\,char.}$ appropriated to the problem, *e.g.* the maximum curvature $\kappa_{\rm m} = \max \left[\boldsymbol{\kappa} \cdot \frac{\nabla v}{|\nabla v|^2} \right]$, and the corresponding radius of curvature

$$R_{\kappa \rm char.} \equiv -\frac{1}{\kappa_{\rm v\,char.}} \frac{1}{\langle B^2 \rangle^{1/2}} \left\langle \frac{B^2}{|\nabla v|^2} \right\rangle^{1/2} . \tag{5}$$

The brackets denote mean values on the closed field line $v = v_0$, $\varphi = \varphi_0$: $\langle B^2 \rangle = \langle B^2 \rangle (v_0, \varphi_0) = \oint B^2 \, d\vartheta / \oint d\vartheta$. In axisymmetric systems, these are equal to the surface averages since all closed lines on a surface are equivalent. The expressions introduced here are convenient when treating general configurations; they reduce to the usual ones when a simple model, e.g. a large aspect-ratio tokamak with circular cross-sections, is invoked.

By balancing the curvature and inertia terms in Eq. (1), one obtains a characteristic growth rate $\gamma_{\rm char.}$, which can be defined as

$$\gamma_{\rm char.}^2 \equiv \frac{2\dot{p}\kappa_{\rm v\,char.}}{\rho} \frac{\langle B^2 \rangle}{\left\langle B^2 / |\nabla v|^2 \right\rangle} = \frac{2p}{\rho R_\kappa L_{\rm p}} = \frac{2c_{\rm s}^2}{R_\kappa L_{\rm p}} \tag{6}$$

where $c_{\rm s} = \sqrt{p/\rho}$ is the thermal velocity and $(1/\dot{\chi}^2) \left\langle B^2 / |\nabla v|^2 \right\rangle \sim {\rm C}^2$ has been used to estimate ${\rm C}^2$. $\gamma_{\rm char.}$ is obviously the characteristic growth rate of ideal ballooning modes.

The field line-tying term in Eq. (1), when reduced by resistivity, tends toward $(4\pi\gamma/\alpha^2 c^2 \eta)\,(d/dy)\,[(1/B^2)\,dF/dy]$. By choosing this term of the same order as the inertia term, one obtains a characteristic number $\alpha_{\rm char.}$ for the transversal variation of the perturbations,

$$\frac{1}{\alpha_{\rm char.}^2} \equiv \frac{c^2 \eta \rho \gamma_{\rm char.}}{\dot{\chi}^4} \left\langle \frac{B^2}{|\nabla v|^2} \right\rangle \frac{L_{\|\rm char.}^2}{L_{\|0}^2} , \tag{7}$$

where (d/dy) has been estimated with a characteristic parallel length, $(d/dy)_{\rm char.} = (\mathbf{B} \cdot \boldsymbol{\nabla})_{\rm char.} / \dot{\chi}(v = v_0, \varphi = \varphi_0) \sim B/(\dot{\chi} L_{\|\rm char.}) \sim 1$. In an equilibrium with cylindrical symmetry, $L_{\|\rm char.}$ is the parallel length corresponding to the imposed periodicity length z_0 in the z-direction; in a tokamak, $L_{\|\rm char.}$ is usually chosen as $L_{\|0}$, though $L_{\|0}/2\pi$ would probably be more appropriate. In a stellerator, $L_{\|\rm char.}$ could be chosen as the width of a local well, or as the width of a less localized well.

The characteristic number $\alpha_{\text{char.}}$ also defines a characteristic scale length L_η,

$$\begin{aligned} L_\eta^2 &\equiv \frac{1}{\alpha_{\text{char.}}^2}\frac{\dot{\chi}^2}{\left\langle B^2/|\nabla v|^2\right\rangle} = \frac{c^2\eta\rho\gamma_{\text{char.}}}{\dot{\chi}^2}\frac{L_{\|\text{char.}}^2}{L_{\|0}^2} \\ &= (2\pi q)^2\left[\frac{\rho e^2\eta R_0\rho_{\text{s}}}{m_{\text{av}}^2\Omega}\right]\left[\frac{2R_0^2}{R_\kappa L_{\text{p}}}\right]^{1/2}\frac{L_{\|\text{char.}}^2}{L_{\|0}^2}\ , \end{aligned} \tag{8}$$

where $\Omega = (ec/m_{\text{av}})\langle B^2\rangle^{1/2}$ and $\rho_{\text{s}} = c_{\text{s}}/\Omega$, with m_{av} the average particle mass and ρ_{s} the gyroradius. Note that $\alpha_{\text{char.}}L_\eta \sim (2\pi r)/q$ in a simple tokamak model with circular cross-sections, local small radius r, $R_\kappa = R_0$ and $L_{\|\text{char.}} = L_{\|0}$.

It is convenient to introduce the scaled mode number $\bar{\mu}$,

$$\bar{\mu} = \alpha/(2\pi\alpha_{\text{char.}})\ , \tag{9}$$

and the scaled growth rate $\mathcal{Q}$,

$$\mathcal{Q} = \gamma/\gamma_{\text{char.}}\ , \tag{10}$$

This scaled growth rate $\mathcal{Q}$ is *not* the same as the growth rate Q often used when studying resistive modes since the latter is defined with respect to the characteristic growth rate of resistive interchanges (see, for example, Ref. [1]).

Equations (1) and (2) can now be written as

$$\begin{aligned} &\frac{\mathrm{d}}{\mathrm{d}y}\left[\frac{1}{\langle\beta\rangle}\frac{R_\kappa L_{\text{p}}}{L_{\|0}^2}\frac{\mathbf{K}^2}{\left[1+\frac{1}{\langle\beta\rangle}\frac{R_\kappa L_{\text{p}}}{L_{\|\text{char.}}^2}\frac{B^2}{\langle B^2\rangle}\frac{4\pi^2\bar{\mu}^2}{\mathcal{Q}}\mathbf{K}^2\right]}\frac{\mathrm{d}F}{\mathrm{d}y}\right] + \frac{1}{\kappa_{\text{v char.}}}\left(\kappa_{\text{v}} + \dot{q}y\kappa_\varphi\right)F \\ &\qquad -\mathcal{Q}^2\mathbf{K}^2F = -\frac{1}{\kappa_{\text{v char.}}}\left(\kappa_{\text{v}} + \dot{q}y\kappa_\varphi\right)D \qquad , \end{aligned} \tag{11}$$

$$\begin{aligned} &\frac{L_{\|\text{char.}}^2}{L_{\|0}^2}\frac{\mathrm{d}}{\mathrm{d}y}\left[\frac{\langle B^2\rangle}{B^2}\frac{\mathrm{d}D}{\mathrm{d}y}\right] - \frac{2}{\gamma_{\text{H}}}\frac{L_{\|\text{char.}}^2}{R_\kappa L_{\text{p}}}\mathcal{Q}^2\left[1+\frac{\gamma_{\text{H}}}{2}\frac{\langle B^2\rangle}{B^2}\langle\beta\rangle\right]D - 4\pi^2\bar{\mu}^2\mathcal{Q}\mathbf{K}^2D \\ &\qquad -\frac{4\pi^2\bar{\mu}^2}{\mathcal{Q}}\frac{1}{\kappa_{\text{v char.}}}\left(\kappa_{\text{v}} + \dot{q}y\kappa_\varphi\right)D = \frac{4\pi^2\bar{\mu}^2}{\mathcal{Q}}\frac{1}{\kappa_{\text{v char.}}}\left(\kappa_{\text{v}} + \dot{q}y\kappa_\varphi\right)F \\ &+4\left[\frac{L_{\|\text{char.}}}{R_\kappa}\right]^2\frac{\mathcal{Q}^2}{\kappa_{\text{v char.}}}\left(\kappa_{\text{v}} + \dot{q}y\kappa_\varphi\right)F \qquad , \end{aligned} \tag{12}$$

where

$$\mathbf{K}^2 \equiv \frac{\dot{\chi}^2}{\left\langle B^2/|\nabla v|^2\right\rangle}\frac{\langle B^2\rangle}{B^2}\mathbf{C}^2 \tag{13}$$

and $\langle\beta\rangle \equiv 8\pi p/\langle B^2\rangle$ have been defined.

The condition

$$L^2_{\|\text{char.}}/(R_\kappa L_\text{p}) >> 1, \tag{14}$$

which usually is very well satisfied near the edge, yields, to leading order,

$$D = 0\ , \tag{15}$$

which is equivalent to neglecting the compressibility effects [6, 7], and only Eq. (11) remains. More details about the parameters involved will be given in Sec. V. It is assumed here that also the inequality

$$\langle\beta\rangle \ll \frac{R_\kappa L_\text{p}}{L^2_{\|\text{char.}}} \ll 1\ . \tag{16}$$

is satisfied. The condition

$$1 << \frac{1}{\langle\beta\rangle}\frac{R_\kappa L_\text{p}}{L^2_{\|\text{char.}}}\frac{B^2}{\langle B^2\rangle}\frac{4\pi^2\bar{\mu}^2}{\mathcal{Q}}\mathbf{K}^2 \tag{17}$$

is equivalent to neglecting the perpendicular magnetic field perturbation; when it is satisfied, the perpendicular perturbation of the magnetic field owing to convection is nearly compensated by magnetic diffusion owing to resistivity, and $(\boldsymbol{\nabla}\times\delta\mathbf{E})_\perp \approx 0$, with $\delta\mathbf{E}$ the electric field perturbation. To lowest order, Eqs. (11) and (12) then yield

$$\frac{\mathrm{d}}{\mathrm{d}y}\left[\frac{\langle B^2\rangle}{B^2}\frac{\mathrm{d}F}{\mathrm{d}y}\right] + \frac{4\pi^2 L^2_{\|0}}{L^2_{\|\text{char.}}}\frac{\bar{\mu}^2}{\mathcal{Q}}\left[\frac{1}{\kappa_{\text{v char.}}}(\kappa_\text{v} + \dot{q}y\kappa_\varphi) - \mathcal{Q}^2\mathbf{K}^2\right]F = 0\ , \tag{18}$$

which, in coordinate-independent form, can be written as

$$\begin{aligned}&\frac{(\mathbf{B}\cdot\boldsymbol{\nabla})}{\dot{\chi}}\left[\frac{\langle B^2\rangle}{B^2}\frac{(\mathbf{B}\cdot\boldsymbol{\nabla})}{\dot{\chi}}F\right] + \frac{4\pi^2 L^2_{\|0}}{L^2_{\|\text{char.}}}\frac{\bar{\mu}^2}{\mathcal{Q}}\left[\frac{\boldsymbol{\kappa}}{\kappa_{\text{v char.}}}\cdot\left[\frac{\boldsymbol{\nabla}v}{|\boldsymbol{\nabla}v|^2} - \frac{\boldsymbol{\nabla}v\times\mathbf{B}}{B^2}\int s\frac{dl}{B}\right]\right.\\ &\left.-\mathcal{Q}^2\frac{\langle B^2\rangle}{\left\langle B^2/|\boldsymbol{\nabla}v|^2\right\rangle|\boldsymbol{\nabla}v|^2}\left[1 + \frac{|\boldsymbol{\nabla}v|^4}{B^2}\left[\int s\frac{dl}{B}\right]^2\right]\right]F = 0\ ,\end{aligned} \tag{19}$$

with the local shear

$$s \equiv \frac{1}{|\boldsymbol{\nabla}v|^4}(\boldsymbol{\nabla}v\times\mathbf{B})\cdot[\boldsymbol{\nabla}\times(\boldsymbol{\nabla}v\times\mathbf{B})]\ , \tag{20}$$

and $(\mathbf{B}\cdot\boldsymbol{\nabla})$ the derivative along the reference line $v = v_0$, $\varphi = \varphi_0$. The integral $\int (s/B)\,dl$ has an arbitrary integration constant $c_0(v_0, \varphi_0)$, which correaponds to the

arbitrariness in choosing the origin of the coordinate y. Equations (18) and (19 are valid not only in cylindrical and axisymmetric configurations, but also in stellarators as long as the inequalities (14) and (16) are satisfied.

The boundary conditions for Eq. (18) are $\lim_{|y|\to\infty} F = 0$. Further, the integrals described in Sec. III. must exist.

III. THE GROWTH RATE $\mathcal{Q}$

General properties of the growth rate $\mathcal{Q}$ can be obtained without explicitly solving Eq. (18). Multiplication of this equation by F^*, the c.c. of F, and integration between $-\infty$ and $+\infty$ results in a quadratic equation for $\mathcal{Q}$ whose solution yields

$$\mathcal{Q}_\pm = \frac{1}{8\pi^2\bar{\mu}^2}\frac{L_{\|\text{char.}}^2}{L_{\|0}^2}\frac{I_{\text{lt}}^2}{I_{\text{i}}^2}\left[-1 \pm \left(1 + 64\pi^4\bar{\mu}^4\frac{L_{\|0}^4}{L_{\|\text{char.}}^4}\frac{I_{\text{i}}^2}{I_{\text{lt}}^4}I_\kappa\right)^{1/2}\right] , \tag{21}$$

where

$$I_{\text{lt}}^2 \equiv \int_\infty^\infty \frac{\langle B^2\rangle}{B^2}\left|\frac{\mathrm{d}F}{\mathrm{d}y}\right|^2 dy , \tag{22}$$

$$I_{\text{i}}^2 \equiv \int_\infty^\infty \mathbf{K}^2\,|F|^2\,dy , \tag{23}$$

$$I_\kappa \equiv \frac{1}{\kappa_{\text{v char.}}}\int_\infty^\infty [\kappa_{\text{v}} + \dot{q}y\kappa_\varphi]\,|F|^2\,dy . \tag{24}$$

Clearly, only the sign of the curvature integral I_κ determines the character of $\mathcal{Q}$.

A. $I_\kappa > 0$

In this case, the two roots $\mathcal{Q}_\pm$ are real and $\mathcal{Q}_+ > 0$, which means instability. Since for all interesting configurations there are always regions of bad curvature, $I_\kappa > 0$ can always be obtained by localizing the perturbations to these regions. The same is not valid in the case of ideal modes because, for localization along $\mathbf{B}$, there is a strong stabilizing effect owing to magnetic field line-tying. It is precisely this effect which is here considerably reduced by resistivity.

B. $I_\kappa < 0,\ 1 + 64\pi^4\bar{\mu}^4 L_{\|0}^4 I_{\text{i}}^2 I_\kappa / \left(L_{\|\text{char.}}^4 I_{\text{lt}}^4\right) > 0$

In this case, both roots $\mathcal{Q}_\pm$ are real and negative (stable).

C. $I_\kappa < 0,\ 1 + 64\pi^4 \bar{\mu}^4 L_{\|0}^4 I_{\mathrm{i}}^2 I_\kappa / \left(L_{\|\mathrm{char.}}^4 I_{\mathrm{lt}}^4\right) < 0$

In this case, both roots $\mathcal{Q}_\pm$ are complex with negative real part (stable).

Therefore, localization of the perturbations along $\mathbf{B}$ around regions of bad curvature always leads to real, positive $\mathcal{Q}$'s. However, the question remains of how strong this localization must actually be to obtain a certain $\mathcal{Q}$.

Although Eq. (21) is useful for deriving general properties of the growth rate, evaluation with arbitrary test functions will not, in general, yield the correct dependence of $\mathcal{Q}$ on η. The actual perturbation must be a solution of the eigenmode equation, Eq. (18), and depends explicitly on $\mathcal{Q}$. Thus, the r.h.s. of Eq. (21) also depends on $\mathcal{Q}$. For this reason, the correct dependence $\mathcal{Q}(\eta)$ was not obtained in Ref. [8]. This can easily be illustrated in cylindrical symmetry.

IV. CYLINDRICAL SYMMETRY

In cylindrical symmetry, the curvature is always destabilizing and $\kappa_{\mathrm{v\,char.}} = \kappa_{\mathrm{v}} = const.$. Based on the usual cylindrical coordinates r, Φ, z, with basis vector $\mathbf{e}_{\mathrm{r}}, \mathbf{e}_\Phi, \mathbf{e}_{\mathrm{z}}$, the Hamada coordinates are given by $v = \pi r^2 z_0$, $\vartheta = \Phi/2\pi$, $\zeta = z/z_0$, where z_0 is the periodicity length in the z-direction. With $\mathbf{B}$ given by $\mathbf{B} = B_\Phi(r)\mathbf{e}_\Phi + B_z(r)\mathbf{e}_{\mathrm{z}}$, one obtains $q = (2\pi r B_z)/(z_0 B_\Phi)$, $R_0 = (z_0 B)/(2\pi B_z)$ and $\kappa_{\mathrm{v\,char.}} = \kappa_{\mathrm{v}} = \boldsymbol{\kappa} \cdot \left(\nabla v / |\nabla v|^2\right) = -r/(q^2 R_0^2 |\nabla v|)$. Evaluation of the vector $\mathbf{K}^2$ yields

$$\mathbf{K}^2 = 1 + \frac{\dot{\chi}^2}{B^2} |\nabla v|^4 \dot{q}^2 y^2 = 1 + \left[2\pi \frac{B_z}{B} S y\right]^2 , \tag{25}$$

where the shear S,

$$S \equiv 2v \frac{\dot{q}}{q} , \tag{26}$$

has been introduced.

Equation (18) can then be written as

$$\frac{\mathrm{d}^2 F}{\mathrm{d}y^2} + \frac{4\pi^2 \bar{\mu}^2}{\mathcal{Q}} \left[1 - \mathcal{Q}^2 \mathbf{K}^2\right] F = 0 , \tag{27}$$

or also

$$\frac{\mathrm{d}^2 F}{\mathrm{d}\hat{y}^2} + \frac{B}{B_z} \frac{\bar{\mu}}{S \mathcal{Q}^{3/2}} \left(1 - \mathcal{Q}^2\right) F - \hat{y}^2 F = 0 , \tag{28}$$

with

$$\hat{y} \equiv 2\pi \left[\frac{B_z}{B} S \bar{\mu} \mathcal{Q}^{1/2}\right]^{1/2} y . \tag{29}$$

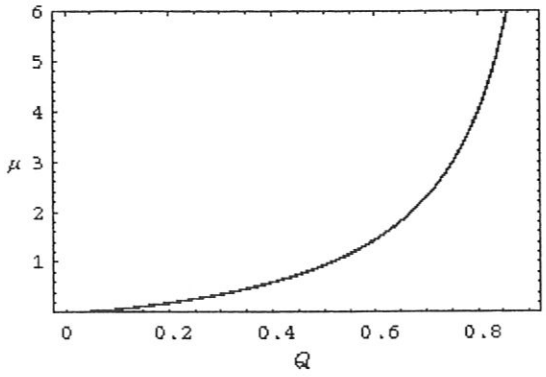

Figure 1: Dispersion relation in cylin. geometry.

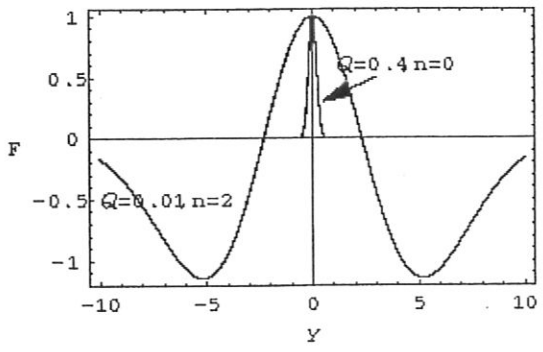

Figure 2: Eigenfunctions in cylindrical geometry.

The solutions which satisfy the boundary conditions are $F_n = H_n(\hat{y}) \exp(-\hat{y}^2/2)$, with $H_n(\hat{y})$ the Hermite polynomial of order n, and $\mathcal{Q}$ given by the dispersion relation

$$\frac{\mathcal{Q}^{3/2}}{1-\mathcal{Q}^2} = \frac{B}{B_z}\frac{\bar{\mu}}{S}\frac{1}{(1+2n)} = \sqrt{1+\left(\frac{2\pi r}{z_0 q}\right)^2}\frac{\bar{\mu}}{S}\frac{1}{(1+2n)} \ , \ n = 0,1,2,\dots \ , \qquad (30)$$

and, therefore,

$$\hat{y} = 2\pi\frac{B_z}{B}S\sqrt{1+2n}\frac{\mathcal{Q}}{\sqrt{1-\mathcal{Q}^2}}y \ . \qquad (31)$$

Because of the symmetry and assumed periodicity in the z-direction, $\alpha \to 2\pi n_z$, with n_z the "toroidal"mode number. Therefore $\bar{\mu} = n_z/\alpha_{\text{char.}}$. The modes with small growth rates $\mathcal{Q}$ decay slowly and are extended along y, while those with large growth rates ($\mathcal{Q} \to 1$) are localized.

Note that n is used here to count the number of nodes of F along $\mathbf{B}$, while n_z or $n_{\text{tor.}}$ is used for the toroidal mode number.

If the r.h.s. of Eq. (30) is small, then $\mathcal{Q}^{3/2} \approx (B\bar{\mu})\,/\,[(1+2n)\,B_z S] \ll 1$, which is the growth rate of resistive interchanges. These modes have $\mathcal{Q} \sim \eta^{1/3}$ and are extended along $\mathbf{B}$ with decay length $y_{\text{d.l.}} \approx B/\left(\sqrt{2(1+2n)}\,\pi B_z S\mathcal{Q}\right)$, a result which was also obtained in Refs. [1, 2], where the general resistive ballooning mode equations were evaluated assuming very small resistivity, an thus $\mathcal{Q} \ll 1$.

When the r.h.s. of Eq. (30) is large, the growth rate becomes independent of η, and $\mathcal{Q} \approx 1$, which is the ideal ballooning growth rate. These modes are localized anywhere along $\mathbf{B}$ with decay length $y_{\text{d.l.}} \approx (B\sqrt{1-\mathcal{Q}})/\left(\pi\sqrt{1+2n}B_z S\right)$, and appear when the stabilizing line-tying effect is considerably reduced by resistivity. However, for large values of $\bar{\mu}$ it might be necessary to take gyroradius effects into account. Figure 1 shows the dispersion relation calculated with $(2\pi r)/z_0 = 0.3$, $q = 3$, $S = 3$, $n = 0$. In Fig. 2, the eigenfunctions corresponding to $\mathcal{Q} = 0.4$, $n = 0$ and $\mathcal{Q} = 0.01$, $n = 2$ are presented.

V. AXIAL SYMMETRY

The details of the derivation of the resistive ballooning mode equation for an axisymmetric, large aspect ratio equilibrium with shifted, circular magnetic surfaces are given in Appendix A. The expansion parameter used is the inverse aspect ratio $\epsilon_M = r/R_M(r)$, with r the small radius of the particular cross-section under consideration, and $R_M(r)$ the distance of its center from the axis of symmetry. Equation (19) then takes the form given by Eq. (A45), which contains the equilibrium quantities ϵ_M, R_M, the safety factor q and the shear S. The perturbation F is described by the scaled mode number $\bar{\mu}$ and the scaled growth rate $\mathcal{Q}$, which, at given $\bar{\mu}$, is the eigenvalue of the mode equation.

The value of the parameters assumed for the calculations are given in detail in Appendix B, and it can be seen that they are consistent with the assumptions made to derive the equations.

Equation (A45), though considerably less complex than the original ballooning equation, is still rather involved. Without claiming rigour, further simplification can be achieved if one discards all small terms, keeping, however, the stabilizing mean toroidal curvature. This is represented here by $-\epsilon$, considered to be a free parameter of order $o(\epsilon_M)$. Under these circumstances, the ballooning equation can be written as

$$\frac{\mathrm{d}^2 F}{\mathrm{d}\Theta^2} + \frac{\bar{\mu}^2}{\mathcal{Q}} \left[-\epsilon + \cos\Theta + S\Theta \sin\Theta - \mathcal{Q}^2 \left(1 + S^2\Theta^2\right) \right] F = 0 \,, \tag{32}$$

to be solved with the boundary conditions $F \to 0$ for $|\Theta| \to \infty$. This equation essentially agrees with results obtained for a similar model within the framework of two-fluid, electrostatic theory when the diamagnetic effects are neglected, as given in Ref. [4], Eq. (20) (with minor discrepancies. In particular, the term $\mathcal{Q}^2$ is given there as $\mathcal{Q}^2/2$), and Ref. [5], Eq. (14). In the last reference the boundary condition are, however, different from those imposed here.

Equation (32) can be solved by analytic approximations when the solutions are assumed to be localized along **B** (as in the cylindrical symmetric case, this turns out to be the case of large growth rates ~ 1), and also when the shear is small. Not being interested in the latter case here, only the first one will be treated analytically.

A. Analytic localized solutions

By assuming that the eigenfunctions decay fastly, and expanding around $\Theta = 0$, Eq. (32) can be written as

$$\frac{\mathrm{d}^2 F}{\mathrm{d}\Theta^2} + \frac{\bar{\mu}^2}{\mathcal{Q}} \left[1 - \epsilon - \mathcal{Q}^2 - \left[1/2 - S + S^2\mathcal{Q}^2 \right] \Theta^2 \right] F = 0 \,, \tag{33}$$

or else

$$\frac{\mathrm{d}^2 F}{\mathrm{d}\hat{\Theta}^2} + \frac{\bar{\mu}}{\mathcal{Q}^{1/2}} \frac{[1-\epsilon-\mathcal{Q}^2]}{[1/2 - S + S^2\mathcal{Q}^2]^{1/2}} F - \hat{\Theta}^2 F = 0 \ , \tag{34}$$

with

$$\hat{\Theta} = \left[\frac{\bar{\mu}^2}{\mathcal{Q}} \left[1/2 - S + S^2\mathcal{Q}^2 \right] \right]^{1/4} \Theta \ , \tag{35}$$

which is Hermite's differential equation if the condition

$$(2S-1)/(2S^2) < \mathcal{Q}^2 < 1 - \epsilon \quad (\text{for } S \geq 1/2), \tag{36}$$

or

$$0 < \mathcal{Q}^2 < 1 - \epsilon \quad (\text{for } S \leq 1/2), \tag{37}$$

is satisfied. The eigenvalues and the eigenfunctions are then

$$\mathcal{Q}^{1/2} \frac{[1/2 - S + S^2\mathcal{Q}^2]^{1/2}}{[1-\epsilon-\mathcal{Q}^2]} = \frac{\bar{\mu}}{(2n+1)} \ , \ n = 0, 1, 2, \ldots , \tag{38}$$

and

$$F_n = H_n(\hat{\Theta_n}) \exp\left[-\frac{\hat{\Theta_n}^2}{2} \right] \ , \tag{39}$$

respectively. Note that in the axisymmetric case the growth rates are bounded from above by $1 - \epsilon$ (in the cylindrical case, by 1) owing to the stabilizing effect of the mean normal curvature $(-\epsilon)$.

B. Numerical solutions

Given the scaled mode number $\bar{\mu}$, Eq. (32) is an eigenvalue equation for the growth rate $\mathcal{Q}$. However, it is more convenient to write

$$\frac{\mathrm{d}^2 F}{\mathrm{d}\Theta^2} + \nu \left[-\epsilon + \cos\Theta + S\Theta \sin\Theta - \mathcal{Q}^2 \left(1 + S^2\Theta^2 \right) \right] F = 0 \ , \tag{40}$$

with

$$\nu \equiv \frac{\bar{\mu}^2}{\mathcal{Q}} \ , \tag{41}$$

and solve for the eigenvalue $\mathcal{Q}$ at given ν. Formulated in this way, Eq. (40), together with the boundary conditions, is a singular *limit point* Sturm-Liouville eigenvalue problem [9], which is solved here using the SLEIGN2 code [10, 11, 12]. After having determined the eigenvalue $\mathcal{Q}$ at given ν, the resulting $\bar{\mu}$, Eqs. (9) and (B3) might not

correspond to an integer value of the poloidal mode number m. This is, however, of no consequence since a very small change in ν, and thus in $\bar{\mu}$, is sufficient to obtain an integer value of m.

For the numerical calculations, a value $\epsilon = 0.3$ is used throughout. Figure 3 shows the dispersion relation for $S = 0.5$ and $n = 0$ (i.e. no zeros of F in $-\infty < \Theta < \infty$), while Figs. 4, 5 and 6 are calculated with $S = 1.0$, $n = 0$, $S = 2.0$, $n = 0$ and $S = 3.0$, $n = 0$, respectively.

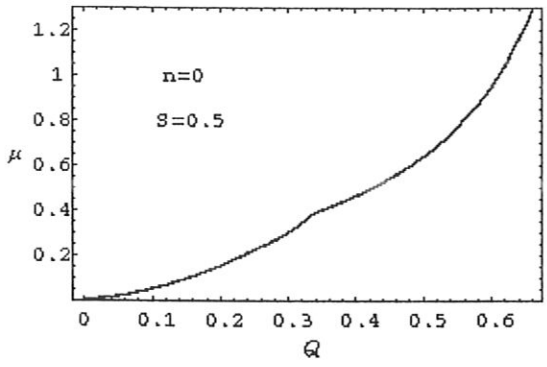

Figure 3: Dispersion relation in axial symmetry for $\epsilon = 0.3$, $S = 0.5$ and $n = 0$.

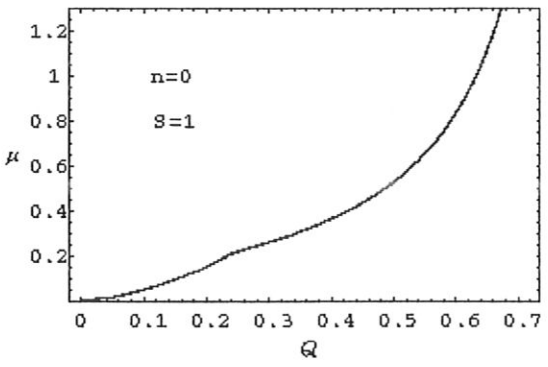

Figure 4: Dispersion relation in axial symmetry for $\epsilon = 0.3$, $S = 1.0$ and $n = 0$.

The effect of shear can better be assessed by drawing the four curves on a single figure. This is done in Fig. 7 and Fig. 8. For small mode numbers ($\bar{\mu} \lesssim 0.1$, $m \lesssim 40$), the shear is not important in the dispersion relation. However, for very small $\bar{\mu}$ and $\mathcal{Q}$, the condition (17) might not be satisfied. In such a case, it is necessary to consider the full equations, Eqs. (11) and (12), and this could modify the results. For higher values of $\bar{\mu}$, the shear is destabilizing. Then, for intermediate values of $\bar{\mu}$, ($\bar{\mu} \gtrsim .25$, $m \gtrsim 95$), it is first destabilizing ($\mathcal{Q}$ increases with S), but becomes stabilizing again when it is further increased ($\mathcal{Q}$ decreases again). Even higher values of $\bar{\mu}$ are stabilized by increasing shear.

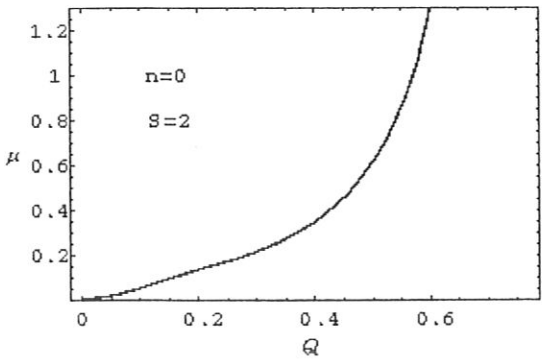

Figure 5: Dispersion relation in axial symmetry for $\epsilon = 0.3$, $S = 2.0$ and $n = 0$

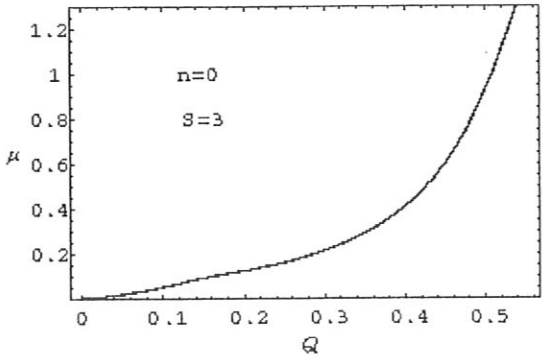

Figure 6: Dispersion relation in axial symmetry for $\epsilon = 0.3$, $S = 3.0$ and $n = 0$

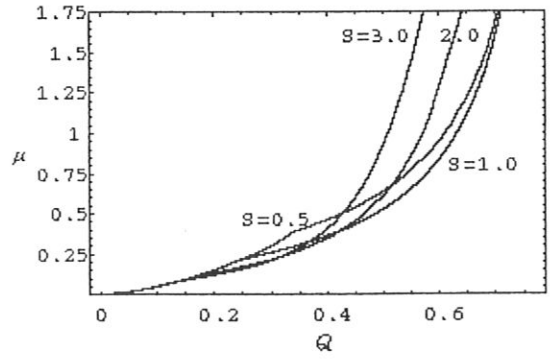

Figure 7: Effect of shear on the dispersion relation

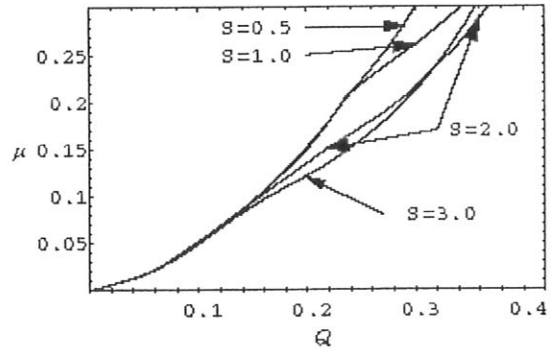

Figure 8: Effect of shear on the dispersion relation

Figures 9, 10 and 11 show the eigenfunction F for $S = 1.0$ and three different values of $\bar{\mu}$, corresponding to the poloidal mode numbers $m = 235$ ($\bar{\mu} = 0.611$), $m = 88$ ($\bar{\mu} = 0.229$) and $m = 49$ ($\bar{\mu} = 0.127$). These pictures show the direct correspondence between the extension of the perturbation along $\mathbf{B}$ and the growth rates: stronger localized perturbations have the larger growth rates. The pictures also show how the perturbations tap the energy from the curvature, becoming large where the curvature is positive, decreasing where it is negative and then vanishing with increasing Θ.

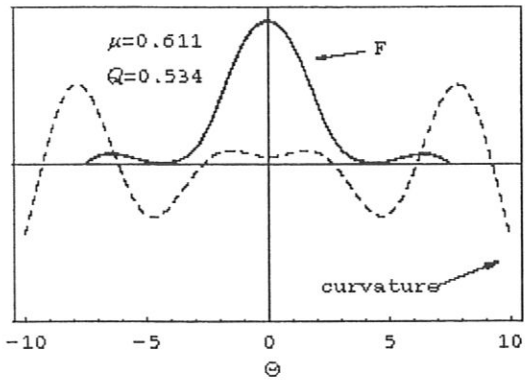

Figure 9: Eigenfunction for $S = 1.0$, $m = 235$ and $n = 0$.

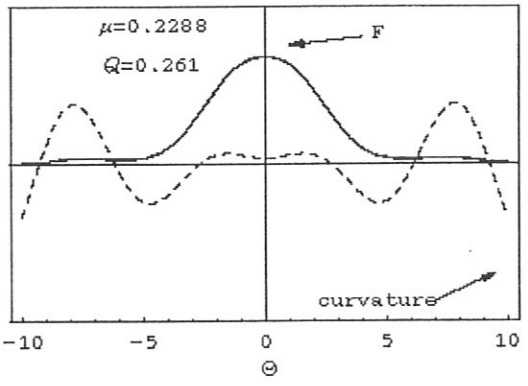

Figure 10: Eigenfunction for $S = 1.0$, $m = 88$ and $n = 0$.

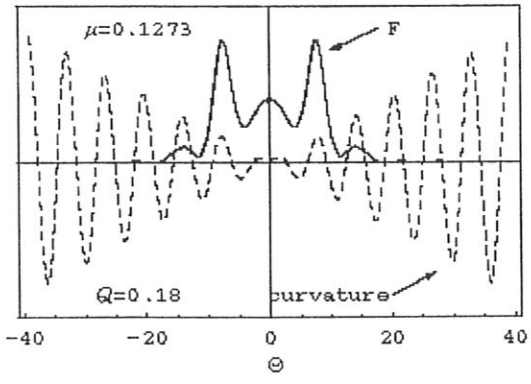

Figure 11: Eigenfunction for $S = 1.0$, $m = 49$ and $n = 0$.

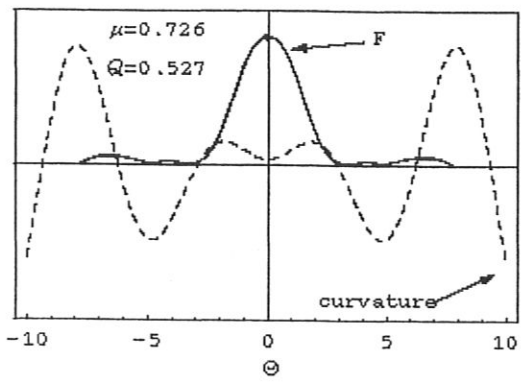

Figure 12: Eigenfunction for $S = 2.0$, $m = 279$ and $n = 0$.

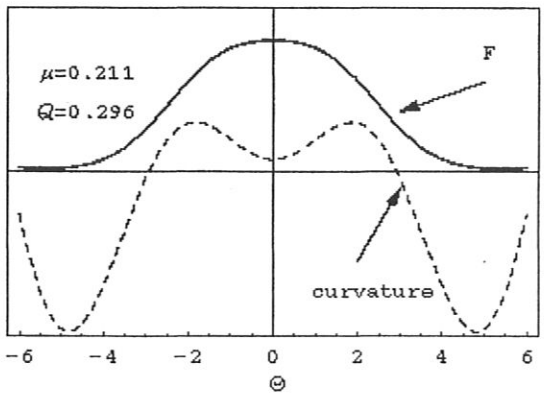

Figure 13: Eigenfunction for $S = 2.0$, $m = 81$ and $n = 0$.

Figures 12 to 15 show the eigenfunction for $S = 2.0$, $n = 0$ and four values of $\bar{\mu}$. The structure becomes more complicated for the extended perturbations, for which the geodetic curvature $\sim S\Theta \sin\Theta$ plays the major role.

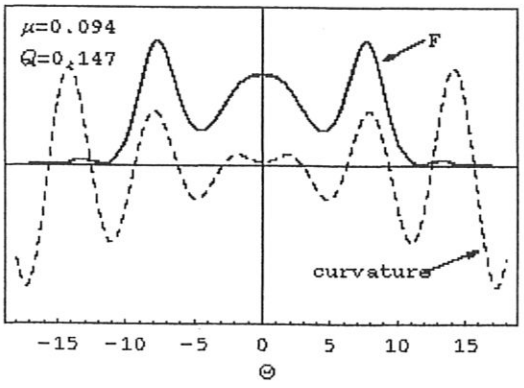

Figure 14: Eigenfunction for $S = 2.0$, $m = 36$ and $n = 0$.

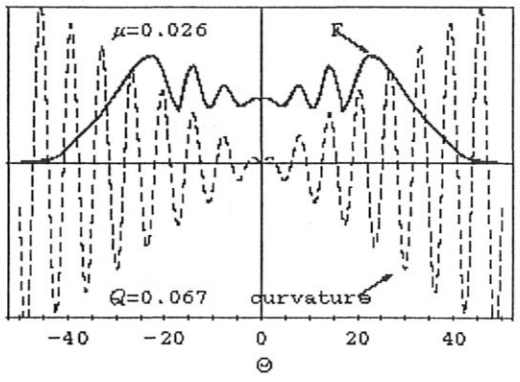

Figure 15: Eigenfunction for $S = 2.0$, $m = 10$ and $n = 0$.

VI. CONCLUSIONS

The resistive ballooning mode equations for general (symmetric as well as non-symmetric) toroidal plasmas have been transformed by introducing space and time length scales which are appropriate for evaluation near the plasma edge of present-day configurations. In many interesting cases, the effect of sound wave propagation can be neglected owing to the low plasma β near the edge, and the two coupled resistive ballooning mode equations reduce to a single one (however, as pointed out in earlier work, the acoustic effects should be included when very small growth rates, $\mathcal{Q} << 1$, are considered.)

Owing to the large resistivity near the edge, the stabilizing effect of the perpendicular magnetic field perturbations is considerably reduced; this makes possible a further simplification of the equations. General properties of the growth rates can then be derived straightforwardly. Unstable solutions are always possible whenever there is a region of unfavourable field line curvature, which is the case for all interesting configurations. The *resistive* growth rates are then comparable to the characteristic growth rates of *ideal* ballooning modes.

A cylindrical plasma and a simple model of an axisymmetric tokamak with shifted, circular cross-sections were studied in detail. Eigenfunctions, growth rates and dispersion relations were calculated both analytically and numerically. The high mode numbers were found to become less unstable with increasing shear, while the low mode numbers are insensitive to shear. The numerical calculations were made taking into account parameters consistent with those of an Asdex Upgrade edge plasma, and for which the resistive ballooning mode effects should dominate over the diamagnetic effects. Finite Larmor radius effects should not be important for the modes considered, which have small or at least moderate values of $\bar{\mu}$ ($k_\perp \rho_{\text{ion}} = 1$ corresponds here to $m = 1000$, $\bar{\mu} = 2.6$.) The modes studied should then play a major role in transport near the plasma edge.

For stellarators, the calculations are much more involved. Since the field lines on a rational surface are not equivalent, contrary to the symmetric cases, evaluation of the resistive ballooning mode equation, Eq. (19) must be done, in principle, for each line. Also, the choice of the origin of the y or Θ coordinates, which was not considered here, could play an important role. This quantity enters the equations as an additional parameter.

APPENDIX A: AXISYMMETRIC CONFIGURATIONS WITH CIRCULAR CROSS-SECTIONS

The quantities needed to evaluate Eq. (18) or Eq. (19) will now be derived for the case of an axisymmetric tokamak with shifted, circular cross-sections, whose geometry is illustrated in Fig.16 .

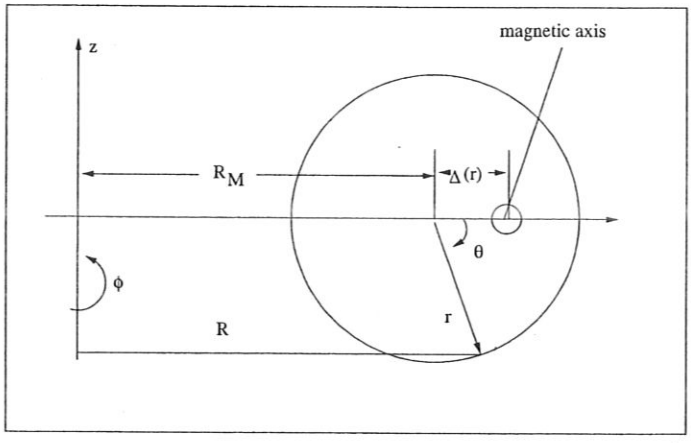

Figure 16: Tokamak with shifted circular surfaces

Let R, Φ, z be the usual cylindrical coordinates with unit basis vectors $\mathbf{e}_R = \cos\Phi\,\mathbf{e}_x + \sin\Phi\,\mathbf{e}_y$, $\mathbf{e}_\Phi = -\sin\Phi\,\mathbf{e}_x + \cos\Phi\,\mathbf{e}_y$ and $\mathbf{e}_z$, where $\mathbf{e}_x$, $\mathbf{e}_y$ and $\mathbf{e}_z$ are the usual Cartesian basis vectors. Let the magnetic axis of the equilibrium be R_A and the geometrical center of a cross-section with small radius r be $R_\mathrm{M}(r)$, shifted by a distance $\Delta(r)$ from R_A. Polar coordinates r, Θ with origin at R_M are defined on the planes of the cross-sections. Then, the distance $R(r,\Theta)$ of a point P from the z-axis is

$$R(r,\Theta) = R_\mathrm{M}(r) + r\cos\Theta = R_\mathrm{A} - \Delta(r) + r\cos\Theta\ , \qquad \text{(A1)}$$

and the radius vector of P is

$$\mathbf{x} = R(r,\Theta)\mathbf{e}_R - r\sin\Theta\,\mathbf{e}_z\ . \qquad \text{(A2)}$$

Denoting derivatives with respect to r by $'$, the coordinate system r, Θ, Φ has the

covariant basis

$$\mathbf{g}_r \equiv \frac{\partial \mathbf{x}}{\partial r} = (R'_{\rm M} + \cos\Theta)\,\mathbf{e}_R - \sin\Theta\,\mathbf{e}_z = \frac{\partial R\,(r,\Theta)}{\partial r}\mathbf{e}_R - \sin\Theta\,\mathbf{e}_z \ , \tag{A3}$$

$$\mathbf{g}_\Theta \equiv \frac{\partial \mathbf{x}}{\partial \Theta} = -r\,[\sin\Theta\,\mathbf{e}_R + \cos\Theta\,\mathbf{e}_z] \ , \tag{A4}$$

$$\mathbf{g}_\Phi \equiv \frac{\partial \mathbf{x}}{\partial \Phi} = R\frac{\partial \mathbf{e}_R}{\partial \Phi} = R\mathbf{e}_\Phi = [R_{\rm M}(r) + r\cos\Theta]\,\mathbf{e}_\Phi \ . \tag{A5}$$

The functional determinant $\mathcal{D}$ is given by

$$\frac{1}{\mathcal{D}} = \mathbf{g}_r \cdot \mathbf{g}_\Theta \times \mathbf{g}_\Phi = rR\,(r,\Theta)\,[1 + R'_{\rm M}\cos\Theta] \ , \tag{A6}$$

and the contravariant basis is given by

$$\boldsymbol{\nabla} r = \mathcal{D}\mathbf{g}_\Theta \times \mathbf{g}_\Phi = \frac{1}{[1 + R'_{\rm M}\cos\Theta]}\,[\cos\Theta\,\mathbf{e}_R - \sin\Theta\,\mathbf{e}_z] \ , \tag{A7}$$

$$\boldsymbol{\nabla}\Theta = \mathcal{D}\mathbf{g}_\Phi \times \mathbf{g}_r = -\frac{1}{r\,[1 + R'_{\rm M}\cos\Theta]}\,[\sin\Theta\,\mathbf{e}_R + [R'_{\rm M} + \cos\Theta]\,\mathbf{e}_z] \ , \tag{A8}$$

$$\boldsymbol{\nabla}\Phi = \mathcal{D}\mathbf{g}_r \times \mathbf{g}_\Theta = \frac{\mathbf{e}_\Phi}{R} = \frac{\mathbf{g}_\Phi}{R^2} \ . \tag{A9}$$

This allows one to calculate the metric coefficients

$$g_{rr} = 1 + 2R'_{\rm M}\cos\Theta + R'^2_{\rm M} \ , \quad g^{rr} = \frac{1}{[1 + R'_{\rm M}\cos\Theta]^2} \ , \tag{A10}$$

$$g_{\Theta\Theta} = r^2 \ , \quad g^{\Theta\Theta} = \frac{[1 + 2R'_{\rm M}\cos\Theta + R'^2_{\rm M}]}{r^2\,[1 + R'_{\rm M}\cos\Theta]^2} \ , \tag{A11}$$

$$g_{\Phi\Phi} = R^2 \ , \quad g^{\Phi\Phi} = 1/R^2 \tag{A12}$$

$$g_{r\Theta} = -rR'_{\rm M}\sin\Theta \ , \quad g^{r\Theta} = \frac{R'_{\rm M}\sin\Theta}{r\,[1 + R'_{\rm M}\cos\Theta]^2} \ . \tag{A13}$$

It is straightforward to derive the following relations which are needed for the curvature:

$$\frac{\partial \mathbf{g}_\Theta}{\partial \Theta} = -r\,[\cos\Theta\,\mathbf{e}_R - \sin\Theta\,\mathbf{e}_z] = -\frac{1}{R\mathcal{D}}\boldsymbol{\nabla} r \ , \tag{A14}$$

$$\frac{\partial \mathbf{g}_\Theta}{\partial \Phi} = -r\sin\Theta\,\mathbf{e}_\Phi = -rR\sin\Theta\,\boldsymbol{\nabla}\Phi \ , \tag{A15}$$

$$\frac{\partial \mathbf{g}_\Phi}{\partial \Theta} = -r\sin\Theta\,\mathbf{e}_\Phi = -rR\sin\Theta\,\boldsymbol{\nabla}\Phi \ , \tag{A16}$$

$$\frac{\partial \mathbf{g}_\Phi}{\partial \Phi} = -R\mathbf{e}_R = -R\boldsymbol{\nabla} R \ . \tag{A17}$$

The general axisymmetric magnetic field can be written as

$$\mathbf{B} = \frac{\dot{\chi}}{2\pi}\boldsymbol{\nabla}\Phi\times\boldsymbol{\nabla} v + f(v)\boldsymbol{\nabla}\Phi \ . \tag{A18}$$

Since $v = 2\pi^2 r^2 R_{\rm M}(r)$ depends only on r, $\mathbf{B}$ can also be expressed as

$$\mathbf{B} = \frac{\chi'}{2\pi}\boldsymbol{\nabla}\Phi\times\boldsymbol{\nabla} r + f(r)\boldsymbol{\nabla}\Phi = \frac{\chi'\mathcal{D}}{2\pi}\mathrm{g}_\Theta + \frac{f}{R^2}\mathrm{g}_\Phi \ , \tag{A19}$$

and

$$B^2 = \left[\frac{\chi'}{2\pi}\right]^2 \frac{g^{rr}}{R^2} + \left[\frac{f}{R}\right]^2 \ . \tag{A20}$$

The derivative along B is

$$(\mathbf{B}\cdot\boldsymbol{\nabla}) = \frac{\chi'\mathcal{D}}{2\pi}\frac{\partial}{\partial\Theta} + \frac{f}{R^2}\frac{\partial}{\partial\Phi} \ . \tag{A21}$$

With these expressions, the calculation of $(\mathbf{B}\cdot\boldsymbol{\nabla})\,\mathbf{B}$ is straightforward. One obtains

$$\begin{aligned}(\mathbf{B}\cdot\boldsymbol{\nabla})\,\mathbf{B} \ = \ & \frac{B^2}{R\left[1+R'_{\rm M}\cos\Theta\right]}\left[-\left[\left[\frac{\Psi'\mathcal{D}R_{\rm M}}{2\pi qB}\right]^2\frac{r}{R_{\rm M}}+\cos\Theta\right]\mathrm{g}_r\right. \\ & \left.+\frac{\sin\Theta}{r}\left[\left[\frac{\Psi'\mathcal{D}R_{\rm M}}{2\pi qB}\right]^2\frac{r^2}{R_{\rm M}^2}R'_{\rm M}\cos\Theta+1\right]\mathrm{g}_\Theta\right] \ .\end{aligned} \tag{A22}$$

The components of the curvature $\boldsymbol{\kappa} = [(\mathbf{B}/B)\cdot\boldsymbol{\nabla}]\,\mathbf{B}/B$ are then

$$\begin{aligned}\frac{\kappa^v}{|\boldsymbol{\nabla} v|^2} \ &= \ \frac{\boldsymbol{\kappa}\cdot\boldsymbol{\nabla} v}{|\boldsymbol{\nabla} v|^2} = \frac{\boldsymbol{\kappa}\cdot\boldsymbol{\nabla} r}{v'\,|\boldsymbol{\nabla} r|^2} \\ &= \ -\frac{\left[1+R'_{\rm M}\cos\Theta\right]}{v'R}\left[\left[\frac{\Psi'\mathcal{D}R_{\rm M}}{2\pi qB}\right]^2\frac{r}{R_{\rm M}}+\cos\Theta\right] \ ,\end{aligned} \tag{A23}$$

$$\begin{aligned}\boldsymbol{\kappa}\cdot\frac{\boldsymbol{\nabla} v\times\mathbf{B}}{B^2} \ &= \ -\frac{v'\mathcal{D}}{B^4}\left[(\mathbf{B}\cdot\boldsymbol{\nabla})\,\mathbf{B}\right]\cdot\left[B_\Phi \mathrm{g}_\Theta\right] \\ &= -\frac{v'B^\Phi}{B^2}\frac{\sin\Theta}{\left[1+R'_{\rm M}\cos\Theta\right]}\left[1+\frac{rR}{R_{\rm M}^2}\frac{R'_{\rm M}}{\left[1+R'_{\rm M}\cos\Theta\right]}\left[\frac{\Psi'\mathcal{D}R_{\rm M}}{2\pi qB}\right]^2\right] \ .\end{aligned} \tag{A24}$$

From the expression for the differential flux $d\Psi(r)$,

$$d\Psi(r) = dr\int_0^{2\pi}\frac{\mathbf{B}\cdot\boldsymbol{\nabla}\Phi}{\mathcal{D}}d\Theta \ , \tag{A25}$$

one obtains

$$\Psi' = \int_0^{2\pi} \frac{B^\Phi}{\mathcal{D}} d\Theta = f \int_0^{2\pi} \frac{1}{\mathcal{D}R^2} d\Theta = 2\pi \frac{f}{R_{\rm M}} \int_0^{2\pi} \frac{[1 + R'_{\rm M} \cos\,\Theta]}{[1 + (r/R_{\rm M}) \cos\,\Theta]} \frac{d\Theta}{2\pi} \ , \qquad \text{(A26)}$$

the safety factor q

$$q = \frac{\Psi'}{\chi'} = \frac{1}{\chi'} \int_0^{2\pi} \frac{B^\Phi}{\mathcal{D}} d\Theta = \frac{f}{\chi'} \int_0^{2\pi} \frac{1}{\mathcal{D}R^2} d\Theta = \frac{2\pi f}{\chi' R_{\rm M}} \int_0^{2\pi} \frac{[1 + R'_{\rm M} \cos\,\Theta]}{[1 + (r/R_{\rm M}) \cos\,\Theta]} \frac{d\Theta}{2\pi} \ , \qquad \text{(A27)}$$

and the relation

$$\begin{aligned} \frac{B^\Phi}{B^\Theta} &= \frac{2\pi f}{\chi' \mathcal{D} R^2} = \frac{f}{\chi'} \int_0^{2\pi} \frac{1}{\mathcal{D}R^2} d\Theta + \frac{2\pi f}{\chi'} \left[\frac{1}{\mathcal{D}R^2} - \frac{1}{2\pi} \int_0^{2\pi} \frac{1}{\mathcal{D}R^2} d\Theta \right] \\ &= q + \frac{2\pi f}{\chi'} \left[\frac{1}{\mathcal{D}R^2} - \frac{1}{2\pi} \int_0^{2\pi} \frac{1}{\mathcal{D}R^2} d\Theta \right] \ . \end{aligned} \qquad \text{(A28)}$$

By expressing $\boldsymbol{\nabla} r$ in terms of covariant basis vectors and multiplying by $\mathbf{B}$, one obtains

$$\boldsymbol{\nabla} r \times \mathbf{B} = \frac{1}{\mathcal{D}} \left[g^{r\Theta} B^\Phi \boldsymbol{\nabla} r - g^{rr} B^\Phi \boldsymbol{\nabla} \Theta + g^{rr} B^\Theta \boldsymbol{\nabla} \Phi \right] \qquad \text{(A29)}$$

and

$$\boldsymbol{\nabla} \times \boldsymbol{\nabla} r \times \mathbf{B} = \boldsymbol{\nabla} \left[\frac{g^{r\Theta} B^\Phi}{\mathcal{D}} \right] \times \boldsymbol{\nabla} r - \boldsymbol{\nabla} \left[\frac{g^{rr} B^\Phi}{\mathcal{D}} \right] \times \boldsymbol{\nabla} \Theta + \boldsymbol{\nabla} \left[\frac{g^{rr} B^\theta}{\mathcal{D}} \right] \times \boldsymbol{\nabla} \Phi \ . \qquad \text{(A30)}$$

After some transformations, these equations yield

$$\frac{1}{|\boldsymbol{\nabla} r|^4} [\boldsymbol{\nabla} r \times \mathbf{B}] \cdot \boldsymbol{\nabla} \times [\boldsymbol{\nabla} r \times \mathbf{B}] = -\frac{\chi'^2 \mathcal{D}}{4\pi^2} \left[\frac{\partial}{\partial r} \left[\frac{B^\Phi}{B^\Theta} \right] + \frac{\partial}{\partial \Theta} \left[\frac{g^{r\Theta}}{g^{rr}} \frac{B^\Phi}{B^\Theta} \right] \right] \ . \qquad \text{(A31)}$$

Assuming $\epsilon_{\rm M} \equiv r/R_{\rm M}(r) \ll 1$ and $R'_{\rm M} \sim o(\epsilon_{\rm M})$, the quantities needed to evaluate the ballooning equation are now calculated to first order in $\epsilon_{\rm M}$. Straightforward expansion yields

$$\frac{1 + R'_{\rm M} \cos\,\Theta}{1 + \epsilon_{\rm M} \cos\,\Theta} = 1 + (-\epsilon_{\rm M} + R'_{\rm M}) \cos\,\Theta + o\left(\epsilon_{\rm M}^2\right) \ , \qquad \text{(A32)}$$

$$\frac{\Psi'}{2\pi f \epsilon_{\rm M}} = 1 + o\left[(\epsilon_{\rm M}^2\right) \ , \qquad \text{(A33)}$$

$$\frac{B^\Phi}{B^\Theta} = q \left[1 + (R'_{\rm M} - \epsilon_{\rm M}) \cos\,\Theta \right] + \cdots \qquad \text{(A34)}$$

$$\frac{r}{q} \left[\frac{B^\Phi}{B^\Theta} \right]' = \frac{rq'}{q} \left[1 + (R'_{\rm M} - \epsilon_{\rm M}) \cos\,\Theta \right] + (R''_{\rm M} r - \epsilon_{\rm M}) \cos\,\Theta + \cdots \ . \qquad \text{(A35)}$$

Since $dl/B = 2\pi d\Theta/(\chi'\mathcal{D})$, one then obtains

$$\int \frac{1}{|\nabla r|^4}[\nabla r \times \mathbf{B}]\cdot\nabla\times[\nabla r\times\mathbf{B}]\frac{dl}{B}$$

$$= \frac{\Psi'}{2\pi r}\left[-\frac{rq'}{q}[\Theta + (R'_{\mathrm{M}} - \epsilon_{\mathrm{M}})\sin\Theta] + (\epsilon_{\mathrm{M}} - R'_{\mathrm{M}} - rR''_{\mathrm{M}})\sin\Theta + \cdots\right] \qquad \text{(A36)}$$

with the arbitrary integration constant (the origin of the Θ or y coordinate) $\Theta_0 = 0$, as seems appropriate for a tokamak with circular cross-sections. The following quantities are also needed:

$$B^2 = \left\langle B^2\right\rangle[1 - 2\epsilon_{\mathrm{M}}\cos\Theta] + \cdots \quad , \quad \left\langle B^2\right\rangle = \frac{f^2}{R_{\mathrm{M}}^2} \, , \qquad \text{(A37)}$$

$$\left[\frac{\Psi'\mathcal{D}R_{\mathrm{M}}}{2\pi qB}\right]^2 = \frac{1}{q^2} + o\left(\epsilon_{\mathrm{M}}^2\right) \qquad \text{(A38)}$$

$$\frac{B^2}{|\nabla r|^2} = \left\langle B^2\right\rangle[1 + 2(R'_{\mathrm{M}} - \epsilon_{\mathrm{M}})\cos\Theta] + \cdots \, , \qquad \text{(A39)}$$

$$\frac{|\nabla r|^4}{B^2} = \left[\frac{2\pi r}{\Psi'}\right]^2[1 + 2(\epsilon_{\mathrm{M}} - 2R'_{\mathrm{M}})\cos\Theta] + \cdots \, . \qquad \text{(A40)}$$

Choosing the characteristic curvature of Sec. II. as

$$\kappa_{\mathrm{v\,char.}} \equiv -\frac{1}{R_{\mathrm{M}}v'} \, , \qquad \text{(A41)}$$

Equations (A23) and (A24) yield

$$\frac{\kappa^v}{|\nabla v|^2} = \kappa_{\mathrm{v\,char.}}\left[\cos\Theta + \frac{\epsilon_{\mathrm{M}}}{q^2} + (R'_{\mathrm{M}} - \epsilon_{\mathrm{M}})\cos^2\Theta\right] + \cdots \qquad \text{(A42)}$$

and

$$\boldsymbol{\kappa}\cdot\frac{[\nabla v\times\mathbf{B}]}{B^2} = \kappa_{\mathrm{v\,char.}}v'^2\frac{2\pi r}{\Psi'}\sin\Theta[1 - R'_{\mathrm{M}}\cos\Theta] + \cdots \, . \qquad \text{(A43)}$$

Since, along the localization line,

$$\frac{\mathbf{B}\cdot\nabla}{\dot{\chi}} = \frac{v'}{2\pi}\mathcal{D}\frac{\partial}{\partial\Theta} = 2\pi[1 - (\epsilon_{\mathrm{M}} + R'_{\mathrm{M}})\cos\Theta]\frac{\mathrm{d}}{\mathrm{d}\Theta} + o\left(\epsilon_{\mathrm{M}}^2\right) \, , \qquad \text{(A44)}$$

the resistive ballooning mode equation, Eq. (19), can be written as

$$\frac{\mathrm{d}}{\mathrm{d}\Theta}\left[[1 + (\epsilon_{\mathrm{M}} - R'_{\mathrm{M}})\cos\Theta]\frac{\mathrm{d}F}{\mathrm{d}\Theta}\right]$$

$$
\begin{aligned}
&+\frac{\bar{\mu}^2}{\mathcal{Q}}\left[1+\left(\epsilon_{\mathrm{M}}+R'_{\mathrm{M}}\right)\cos\Theta\right]\left[\cos\Theta-\epsilon_{\mathrm{M}}\left(1-\frac{1}{q^2}\right)+R'_{\mathrm{M}}+rR''_{\mathrm{M}}\sin^2\Theta\right.\\
&+S\sin\Theta\left[\Theta\left(1-R'_{\mathrm{M}}\cos\Theta\right)+\left(R'_{\mathrm{M}}-\epsilon_{\mathrm{M}}\right)\sin\Theta\right]\\
&-\mathcal{Q}^2\left[1+S^2\Theta^2+2\left(\epsilon_{\mathrm{M}}-R'_{\mathrm{M}}\right)S^2\Theta^2\cos\Theta\right.\\
&\left.\left.+2\left[\left(R'_{\mathrm{M}}-\epsilon_{\mathrm{M}}\right)\left(1+S\right)+rR''_{\mathrm{M}}\right]S\Theta\sin\Theta+2R'_{\mathrm{M}}\cos\Theta\right]\right]F=0\ , \qquad \text{(A45)}
\end{aligned}
$$

where $L_{\|\mathrm{char.}}=L_{\|0}$ (as is appropriate for a tokamak) has been used, and where S is the shear as defined by Eq. (26), $S=2v\dot{q}/q=rq'/q+o\left(\epsilon_{\mathrm{M}}^2\right)$.

APPENDIX B: PLASMA PARAMETERS FOR THE AXISYMMETRIC CASE

For the axisymmetric case, the plasma edge parameters are chosen to be consistent with those of Asdex Upgrade [13, 14] and are shown in Table 1.

Large plasma radius	$R_0 = 165cm$
Small plasma radius	$a = 50cm$
Small radius of reference surface	$r = 48cm$
Aspect ratio ϵ_a	$\epsilon_a = 0.3$
Aspect ratio ϵ_r	$\epsilon_r = 0.29$
Safety factor	$q = 3$
Electron temperature	$T_e = 40eV$
Ion temperature	$T_i = 40eV$
Electron density	$n_e = 2 \times 10^{13}/cm^3$
Ion density	$n_i = 2 \times 10^{13}/cm^3$
Ion mass	$m_i = 2m_{proton}$
Effective charge	$Z_{eff} = 2.5$
Magnetic field	$2.5 \times 10^4 gauss$
Density decay length	$L_n = 4cm$
Temperature decay length	$L_T = 4cm$
Pressure decay length	$L_p = 2cm$
$\epsilon_n \equiv (2L_n)/R_0$	$\epsilon_n = 0.05$

Table 1: Edge plasma parameters.

For the shear, the values $S = 1$ and $S = 2$ are used in the numerical calculations. With the help of Table 1, it is straightforward to calculate further quantities needed. These are given in Table 2. In axial symmetry, the mode number α, the toroidal mode number $n_{tor.}$, the poloidal mode number m and the poloidal wave number k_θ are related by the following expressions:

$$\alpha = 2\pi n_{tor.} = 2\pi m/q = 2\pi r k_\theta/q \ . \tag{B1}$$

The characteristic drift frequency is then

$$\omega_{*char.} = \frac{cT_e}{eB}\frac{n_e'(r)}{n_e}k_{\theta char.} = \frac{\rho_s c_s}{L_n}\frac{\alpha_{char.}q}{2\pi r} = \frac{\rho_s c_s}{L_n L_\eta} \ . \tag{B2}$$

Resistivity	$\eta = 1,45 \times 10^{-15} sec$
Mean thermal velocity	$c_s = 0.62 \times 10^7 cm/sec$
Electron gyrofrequency	$\Omega_e = 4.4 \times 10^{11}/sec$
Ion gyrofrequency	$\Omega_i = 1.2 \times 10^8/sec$
Ion gyroradius	$\rho_i = 0.05cm$
Local plasma β	$\beta = 10^{-4}$
Characteristic growth rate	$\gamma_{char.} = 0.48 \times 10^6/sec$
Characteristic drift frequency	$\omega_{*char.} = 0.98 \times 10^5/sec$
Characteristic resistive length	$L_\eta = 0.79cm$
$\alpha_* \equiv \omega_{*char.}/\gamma_{char.}$	$\alpha_* = 0.2$

Table 2: Calculated equilibrium and characteristic quantities.

Since $\alpha_* = 0.2$ and $\epsilon_n = 0.05$, one is in a region of parameter space where the resistive ballooning modes are dominant [3].

The relation between the scaled mode number $\bar{\mu}$ and the poloidal mode number m is

$$\bar{\mu} = \frac{1}{2\pi}\frac{\alpha}{\alpha_{char.}} = \frac{m}{2\pi}\frac{L_\eta}{r} = 0.0026m \ . \tag{B3}$$

*

References

[1] D. Correa-Restrepo, Z. Naturforsch. **37a**, 848 (1982).

[2] D. Correa-Restrepo, in *Plasma Physics and Controlled Nuclear Fusion Research 1982*, volume II, pages 519–530, International Atomic Energy Agency, Vienna, 1983.

[3] A. Zeiler, D. Biskamp, J. F. Drake, and B. N. Rogers, Phys. Plasmas **5**, 2654 (1998).

[4] S. V. Novakovskii, P. N. Guzdar, J. F. Drake, C. S. Liu, and F. L. Waelbroeck, Phys. Plasmas **2**, 781 (1995).

[5] S. V. Novakovskii, P. N. Guzdar, J. F. Drake, and C. S. Liu, Phys. Plasmas **2**, 3764 (1995).

[6] D. Correa-Restrepo, Z. Naturforsch. **45a**, 609 (1990).

[7] H. Wobig and R. A. Scardovelli, in *Proc. of the Joint Varenna-Lausanne Workshop on Theory of Fusion Plasmas*, volume I, pages 103–11, Scietà Italiana di Fisica, 1989.

[8] G. Bateman and D. B. Nelson, Phys. Rev. Lett **41**, 1804 (1978).

[9] I. Stakgold, *Green's Functions and Boundary Value Problems*, page 438, John Wiley & Sons, New York, 1979.

[10] P. B. Bailey, W. N. Everitt, and A. Zettl, Results in Mathematics **20**, 391 (1991).

[11] P. B. Bailey, W. N. Everitt, J. Weidmann, and A. Zettl, Results in Mathematics **23**, 3 (1993).

[12] P. B. Bailey, W. N. Everitt, and A. Zettl, Proc. Roy. Soc. of Edinburgh **126A**, 505 (1996).

[13] ASDEX Team, Nucl. Fusion **29**, 1959 (1989).

[14] W.Suttrop, H. J. de Blank, G. Haas, H. Murmann, O. Gehre, H. Reimerdes, F. Ryter, H. Salzmann, J. Schweinzer, J. Stober, H. Zohm, ASDEX Upgrade team, NBI team and ICRH team, in *Proceedings of the 23rd European Physical Society Conference on Controlled Fusion and Plasma Physics, Kiev*, volume I, pages 47–50, European Physical Society, Petit-Lancy, 1996.